

See discussions, stats, and author profiles for this publication at: <https://www.researchgate.net/publication/45628253>

Mechanistic Insights into Cu(I)-Catalyzed Azide-Alkyne "Click" Cycloaddition Monitored by Real Time Infrared Spectroscopy

ARTICLE *in* THE JOURNAL OF PHYSICAL CHEMISTRY A · AUGUST 2010

Impact Factor: 2.69 · DOI: 10.1021/jp105034m · Source: PubMed

CITATIONS

30

READS

29

2 AUTHORS:



Shengtong Sun

Universität Konstanz

27 PUBLICATIONS 646 CITATIONS

SEE PROFILE



Peiyi wu

Fudan University

218 PUBLICATIONS 3,616 CITATIONS

SEE PROFILE

Mechanistic Insights into Cu(I)-Catalyzed Azide–Alkyne “Click” Cycloaddition Monitored by Real Time Infrared Spectroscopy

Shengtong Sun and Peiyi Wu*

The Key Laboratory of Molecular Engineering of Polymers, Ministry of Education, Department of Macromolecular Science, and Laboratory of Advanced Materials, Fudan University, Shanghai 200433, People's Republic of China

Received: June 1, 2010; Revised Manuscript Received: July 14, 2010

A designed ligand-accelerated Cu(I)-catalyzed cycloaddition (CuAAC) reaction was monitored for the first time by real time infrared analysis technique based on ATR-FTIR principles. Principal components analysis (PCA) and two-dimensional correlation spectroscopy (2Dcos) results showed that the consumption of alkyne and azide took place successively followed by the formation of the product 1,2,3-triazole, and a 1:1 complex of two reactants would be formed in the reaction process. The rate-determining step of the CuAAC reaction was also experimentally confirmed for the first time to be the transition of azide–alkyne 1:1 complex to the preproduct 1,2,3-triazole. Our results are in good conformity with the current catalytic mechanism proposed by Sharpless et al. according to DFT calculation results.

1. Introduction

As natural molecules have an overall preference for carbon–heteroatom bonds, in contrary to our focus on organic synthesis by carbon–carbon bonding nowadays, click chemistry serves as a rather powerful strategy in request for function with highly energetic “spring-loaded” reactants.¹ Of all the reactions in the scope of click reaction, Cu(I)-catalyzed Huisgen 1,3-dipolar azide–alkyne cycloaddition to yield 1,4-regioselective 1,2,3-triazoles² is undoubtedly the most powerful and representative one discovered to date. This reaction can succeed with high yields, purity, and reaction rate (up to 10⁷ times) over a broad temperature range (0–160 °C) and pH range (ca. 4–12) and in the presence of the majority of organic synthesis conditions and functional groups.³ In other words, Cu(I)-catalyzed azide–alkyne cycloaddition (CuAAC) is a very robust reaction which has opened growing applications in bioconjugation, organic synthesis, materials and surface science, polymer science, etc.⁴

In spite of increasing studies on the applicability of CuAAC, deep mechanistic understanding of the overall features of this unique catalytic process appears much more difficult, due to its “incredible” and “perfect” selectivity, reactivity, and reliability, which mainly involve multiple on- and off-cycle equilibria, formation of ill-defined and catalytically incompetent copper acetylide aggregates. Several investigations devoted to comprehend the mechanism of CuAAC have been reported recently by performing kinetics studies either for ligand-free⁵ or for ligand-accelerated⁶ CuAAC reactions, and some of its derivative reactions such as cyclodimerization⁷ and Cu(I)-catalyzed click step-growth polymerization⁸ are also very helpful to achieve a better understanding of CuAAC. It is worth noting that nearly all of the current mechanistic interpretations are based on the results proposed by Sharpless et al., who predicted unprecedented reactivity and intermediates of CuAAC via a DFT study.⁹ Compared to the thermally induced Huisgen 1,3-dipolar cycloaddition with a confirmed uncatalyzed concerted mechanism, CuAAC would adopt a stepwise annealing pathway to

afford regioselective 1,4-substituted 1,2,3-triazoles. However, concerted direct pathway cannot explain Cu(I)-catalyzed accelerating effect due to a too high barrier. Thus, two intermediates with much lower barriers were proposed to account for this problem. Nevertheless, there is still no experimental proof for its key steps and intermediates.

Herein, we report our mechanistic results from monitoring a designed ligand-accelerated CuAAC reaction for the first time by real time infrared analysis technique based on ATR-FTIR principles. Unlike other online techniques, such as LC-MS,^{5,6b} NMR,⁸ or UV–vis¹⁰ with inextricable time delay, operation inconvenience, and, mostly important, lack of direct response to all reacting species, IR spectroscopy is very suitable for real time monitoring of various chemical processes such as catalysis, crystallization, organic/inorganic chemistry, pharmaceutical/biological analysis, polymerization, etc.¹¹ In this paper, two powerful qualitative methods, chemometrics¹² and two-dimensional correlation spectroscopy (2Dcos),¹³ were also used to extract primary spectral information in order to experimentally evaluate the rationality of the current mechanism by discerning the sequence order of different reaction species and searching for possible intermediates.

2. Experimental Section

2.1. Materials. Sodium azide (NaN₃), propargyl alcohol, and copper bromide (CuBr) were purchased from Aladdin Co. Ltd., and CuBr was purified by washing several times with methanol. *N,N,N',N',N''*-Pentamethyldiethylenetriamine (PMDETA, 98%) was obtained from J&K Chemical Ltd. and used as received. Benzyl bromide, acetic acid, and dimethylformamide (DMF) were all purchased from Sinopharm Chemical Reagent Co. Ltd., and only DMF was purified by vacuum distillation before use. Unless stated otherwise, other reagents and solvents were all purchased from commercial suppliers and were used without further purification.

2.2. Instruments and Measurements. Time-resolved online ATR-FTIR spectra were recorded on a ReactIR 45 m spectrometer (Mettler-Toledo) equipped with a silicon probe with a resolution of 8 cm^{−1} and 32 scans. After the probe was fixed

* Corresponding author. E-mail: peiyiwu@fudan.edu.cn.

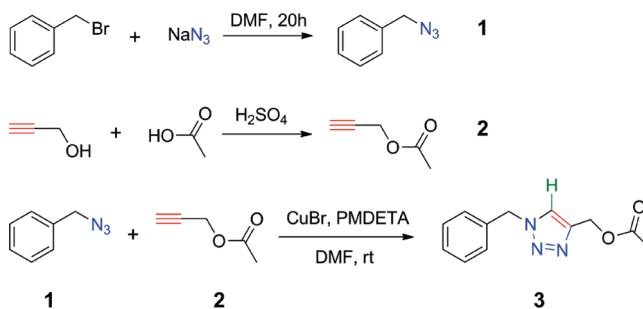
and all of the reactants were added, each spectrum was collected immediately at intervals of 1 min under the protection of nitrogen. An even agitation should be maintained to avoid bringing bubbles onto the surface of the probe, which would lead to a large intensity decrease of IR spectra. FTIR spectra of pure components were measured on a Nicolet Nexus 470 spectrometer with a resolution of 4 cm^{-1} and 64 scans. ^1H and ^{13}C NMR spectra were recorded on Varian Mercury plus 400 M spectrometer with CDCl_3 as solvent and TMS as the internal reference. Elemental analysis was performed on VARIO EL3 instrument (ELEMENTAR, Germany). The melting point (mp) was measured on a Mettler-Toledo differential scanning calorimeter thermal analyzer at a heating rate of 10 $^\circ\text{C}/\text{min}$ from 0 to 70 $^\circ\text{C}$.

2.3. Synthesis Procedure. **2.3.1. Synthesis of Benzyl Azide 1 and Propargyl Acetate 2.** Benzyl azide was synthesized as described previously.⁸ The mixture of benzyl bromide (8.77 g, 0.051 mol) and sodium azide (10 g, 0.154 mol) in 50 mL of DMF was stirred in the dark for 20 h at room temperature. After filtration of NaBr and NaN_3 salts and addition of 50 mL of water, the product was extracted with diethyl ether (3 \times 25 mL). Then the solution was dried with anhydrous Na_2SO_4 overnight, and concentrated residue was further purified by column chromatography with diethyl ether as the eluting solvent to afford **1** as a colorless liquid (4.72 g, 70%). ^1H NMR (CDCl_3): δ 7.36 (m, 5H, C_6H_5 —), δ 4.35 (s, 2H, $-\text{CH}_2-$). ^{13}C NMR (CDCl_3): δ 135.6, 129.1, 128.6, 128.5, 55.0. IR: 2100 cm^{-1} ($-\text{N}_3$).

2.3.2. Synthesis of Propargyl Acetate 2. The mixture of propargyl alcohol (25 mL, 0.424 mol) and acetic acid (26 mL, 0.455 mol) was stirred vigorously overnight at room temperature after adding 7–8 drops of concentrated H_2SO_4 . Then 100 mL of 5% Na_2CO_3 aqueous solution was added, and the product was extracted by dichloromethane (3 \times 50 mL), washed to neutral with water. After drying with anhydrous Na_2SO_4 overnight, the solvent was removed to afford **2** as a colorless liquid (9.7 g). ^1H NMR (CDCl_3): δ 4.68 (d, 2H, $-\text{CH}_2-$), 2.53 (t, 1H, $\equiv\text{C}-\text{H}$), 2.11 (s, 3H, $-\text{CH}_3$). ^{13}C NMR (CDCl_3): δ 170.3, 77.8, 75.1, 20.9. IR: 3300 cm^{-1} ($\equiv\text{C}-\text{H}$), 2135 cm^{-1} ($\text{C}\equiv\text{C}$).

2.3.3. General Procedure for Cu(I)-Catalyzed Synthesis of 1,4-Disubstituted 1,2,3-Triazole 3. For [azide]/[alkyne] = 1/1, benzyl azide **1** (0.5 g, 3.76 mmol), CuBr (0.0108 g, 0.075 mmol), and PMDETA (31 μL , 0.15 mmol) were mixed in 10 mL of DMF first, and then propargyl acetate **2** (0.368 g, 3.76 mmol) was added into the solution. The Cu(I)-catalyzed cycloaddition reaction proceeded at room temperature (20 $^\circ\text{C}$) under nitrogen protection for ca. 40 min and was real time monitored by ReactIR throughout the process. After the reaction finished, the reaction solution was diluted by a spot of DMF and passed through a short alumina column to remove the catalyst. After adding 20 mL of water to dissolve the solution, the product was extracted with diethyl ether (3 \times 25 mL) and dried with anhydrous Na_2SO_4 overnight. To obtain the pure product for spectral comparison, concentrated residue was purified by column chromatography with diethyl ether as the eluting solvent. After further recrystallization twice, a white crystalline solid **3** (0.68 g, 78%) was obtained: mp 58–59 $^\circ\text{C}$. ^1H NMR (CDCl_3): δ 7.51 (s, 1H, H in triazole), 7.40–7.36 (m, 3H, *m*, *p*-H in C_6H_5 —), 7.29–7.27 (m, 2H, *o*-H in C_6H_5 —), 5.52 (s, 2H, $-\text{CH}_2-$ close to phenyl), 5.18 (s, 2H, $-\text{CH}_2-$ close to ester), 2.05 (s, 3H, $-\text{CH}_3$). ^{13}C NMR (CDCl_3): δ 171.1, 143.6, 134.6, 129.4, 129.1, 128.4, 123.8, 57.8, 54.5, 21.1. Anal. Calcd: C, 62.33; H, 5.67; N, 18.17. Found: C, 62.49; H, 5.98; N, 18.23. IR: 3130 cm^{-1} (C–H in triazole).

SCHEME 1: Designed Ligand-Accelerated Cu(I)-Catalyzed Azide–Alkyne Cycloaddition Reaction



For [azide]/[alkyne] = 1/2 and 2/1, only the amount of alkyne and azide was changed to 0.732 and 1.0 g, respectively, and other reacting and measuring conditions were all the same.

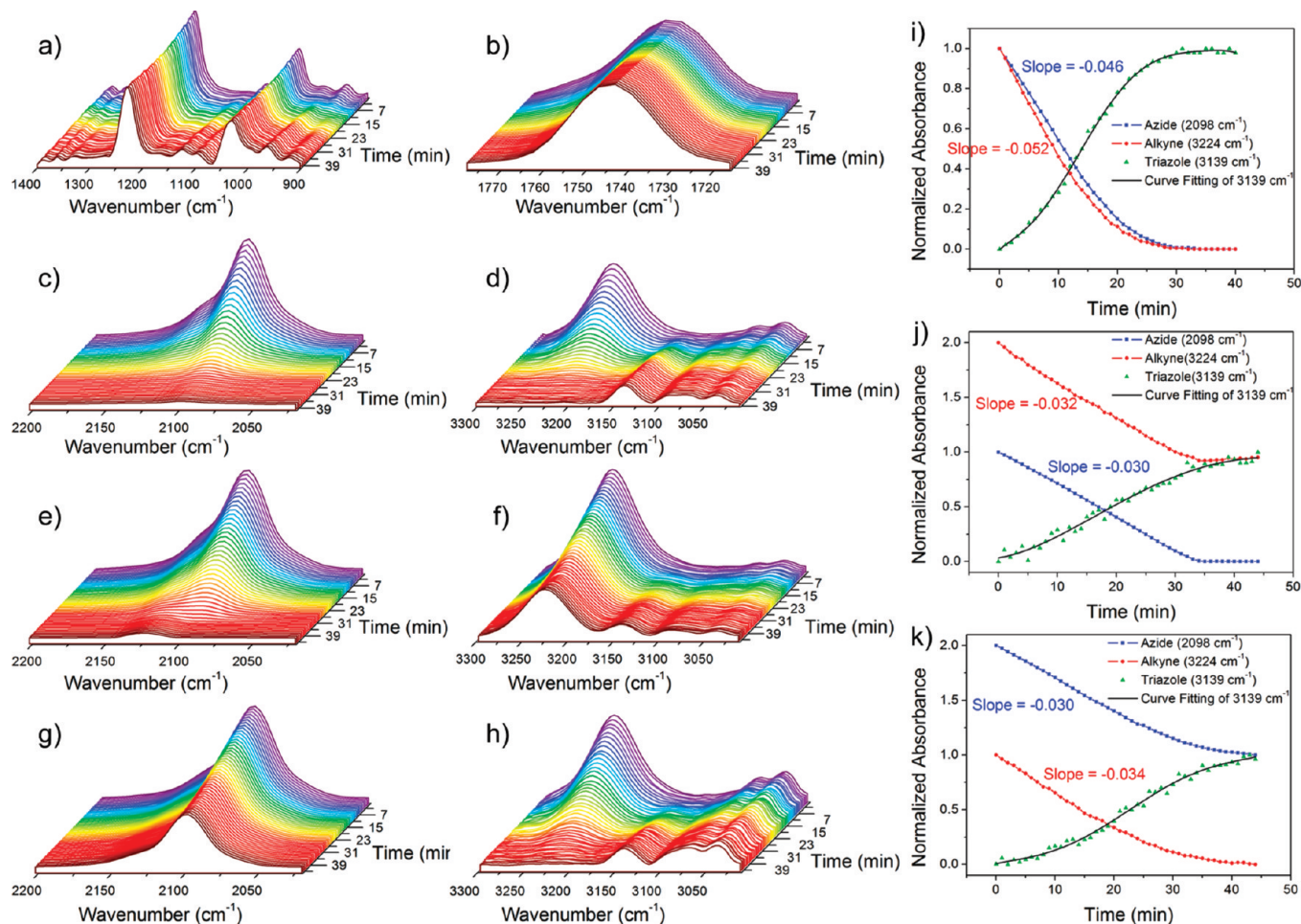
2.4. Investigation Methods. **2.4.1. Principal Component Analysis.** After subtracting the solvent spectrum and baseline correcting, all ATR-FTIR spectra at the 1:1 molar ratio of reactants with an increment of 1 $^\circ\text{C}$ were used to perform principal component analysis (PCA) calculation by the software The Unscrambler ver. 9.7 (CAMO Software AS, 1986–2007). The data set used for PCA was mean centered in advance.

2.4.2. Two-Dimensional Correlation Spectroscopy. PCA-reconstructed ATR-FTIR spectra at the time range of 0–40 min were used to perform 2D correlation analysis. The 2D correlation analysis was carried out using the software 2D Shige ver. 1.3 (Shigeaki Morita, Kwansei-Gakuin University, Japan, 2004–2005) and was further plotted into the contour maps by Origin program ver. 8.0. In the contour maps, warm colors (red and yellow) are defined as positive intensities, while cool colors (blue) are negative ones.

3. Results and Discussion

The designed ligand-accelerated CuAAC reaction (Scheme 1) was real time monitored by a Mettler-Toledo ReactIR instrument equipped with a silicon ATR probe (Figure 1). The solvent (DMF) spectrum has been subtracted to enhance the signal of reaction species. Four regions were the focus in this paper: region 3300–3010 cm^{-1} , where C–H stretching vibrations in alkynyl and 1,2,3-triazole locate; region 2200–2020 cm^{-1} , where the stretching vibration of $-\text{N}-\text{N}\equiv\text{N}$ in azido locates; region 1780–1715 cm^{-1} , where C=O stretching vibration locates; and the fingerprint region 1400–900 cm^{-1} . To further investigate the effect of reactant concentration on the reaction dynamics, another two experiments with excess alkyne and azide were also performed.

From Figure 1c–h, the decreasing of characteristic peaks at 3224 and 2098 cm^{-1} of alkyne and azide and the increasing of the characteristic peak at 3139 cm^{-1} of 1,2,3-triazole can be easily observed. We plotted absorbance–time curves (Figure 1i–k) and found that the two reactants both showed a linear decrease of concentration (represented by absorbance) at the beginning of the reaction and a gradually decreasing consuming rate after a period of time, while the product or 1,2,3-triazole exhibited an “S-shaped” increase. Similar discontinuous kinetic profile has also been observed by Nishimura et al.,¹⁴ who attributed it to the result of the formation of tris-triazole. Judging from the slopes of the two reactants, we concluded that alkyne always had a slightly higher consuming rate than azide, no matter what the molar ratio was. Furthermore, under conditions of little Cu(I) (1/50 of reactants), a deviation from 1:1 ratio of reactants would induce the decrease of reacting rate, indicating



that azide and alkyne may form a 1:1 complex in the reacting process. The formation of azide–alkyne 1:1 complex can also be supported by their same changing reaction rate orders roughly determined by $\ln(-dA/dt) - \ln A$ scatter plots (as for 1:1 molar ratio, alkyne, $0 \rightarrow 0.62$; azide, $0 \rightarrow 0.59$; see Supporting Information for details). It is in good conformity with the stepwise mechanism proposed by Sharpless et al. In addition, excess alkyne would lead to longer period of linearly consuming tendency of the two reactants, indicating that the complexation of alkyne and azide was mainly controlled by the concentration of alkyne. This also supports the current mechanism in which alkyne would first coordinate with Cu(I) before the formation of 1:1 complex with azide. As the product (1,2,3-triazole) with S-shaped increasing had an accelerating process at the beginning of the reaction, we can primarily deduce the sequence of different reacting species as follows (\rightarrow means prior to or earlier than): consumption of alkyne \rightarrow consumption of azide \rightarrow formation of 1,2,3-triazole.

The fingerprint region 1400–900 cm^{-1} (Figure 1a) is rather complicated and hard to analyze. However, this region contains much more spectral information about subtle structural changes, which is very suitable for chemometrics analysis. Principal component analysis (PCA) was employed in this paper. Interestingly, there are only two principal components generated here, wherein the first principal component (PC-1) can explain 75% of spectra variation, while the second principal component (PC-2) can explain 23% of spectra variation.

From the loadings plots of these two components in Figure 2c,d, we can determine that PC-1 should arise from the

contribution of the product 1,2,3-triazole and PC-2 from the combining contributions of the two reactants. It should be noted that PCA always undergoes a mean-centered pretreatment, and only if two components have a strict stoichiometric relationship or linear functional relationship, there would be only one component left because it is necessary to describe all of the spectral variation with one component. The number of components calculated from PCA revealed that CuAAC reaction is a strict stoichiometric reaction, and the spectral combination of the two reactants indicates that azide and alkyne should have formed a 1:1 complex, which accounted for the second principal contribution to spectral variation. However, considering there is no obvious deviation of spectral changes of azido and alkynyl stretching vibrations and no new bands formed at any time points (Figure 1), we contributed this 1:1 complex to the slightly complexing intermediate (**6** in Scheme 2).

The score changes of PC-1 in Figure 2a is easy to understand, similar to the characteristic peak intensity variation of 1,2,3-triazole in Figure 1i. However, the score changes of PC-2 underwent mainly three stages, which can be easily observed in the scatter plot in Figure 2b. Before 11 min, PC-2 or the intermediate (1:1 complex) and PC-1 or 1,2,3-triazole gradually formed. At 12–29 min, the concentration of PC-2 or the intermediate is nearly unchanged, while the formation of PC-1 or 1,2,3-triazole reached the maximum. In other words, at this stage, the consumption of alkyne and azide and the formation of 1,2,3-triazole approached a balance. At the last stage between 30 and 40 min, alkyne and azide had been totally consumed, and then the intermediate was largely consumed causing obvious

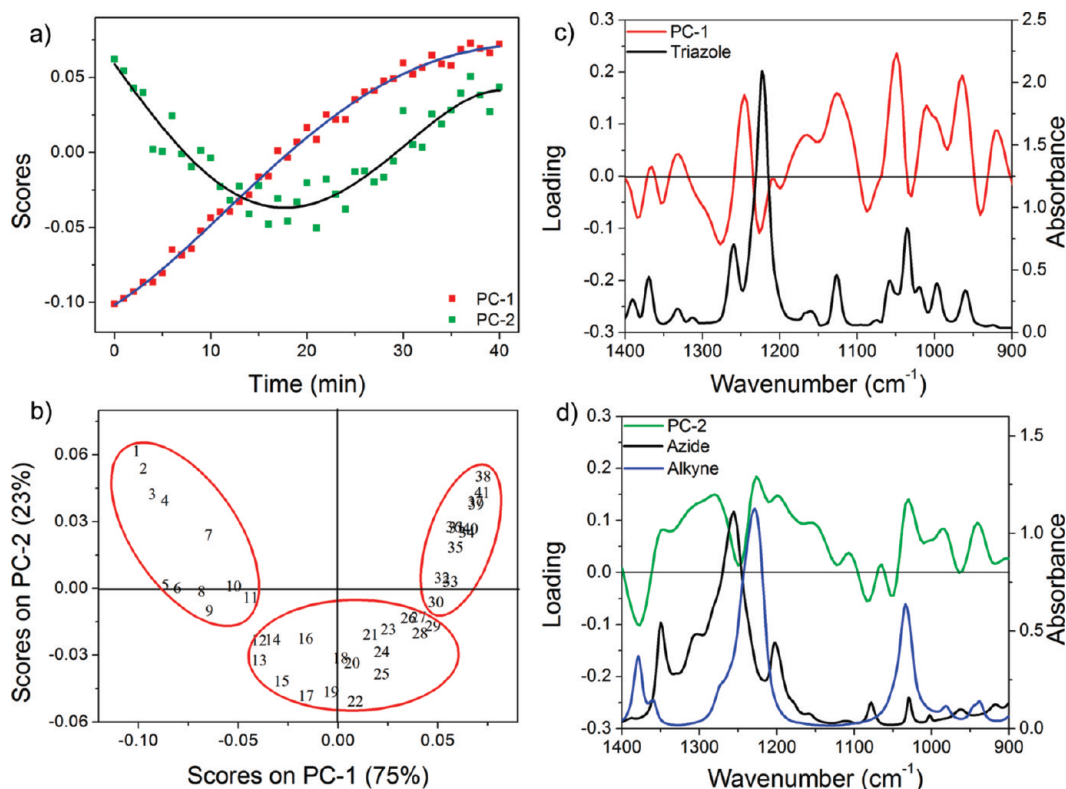
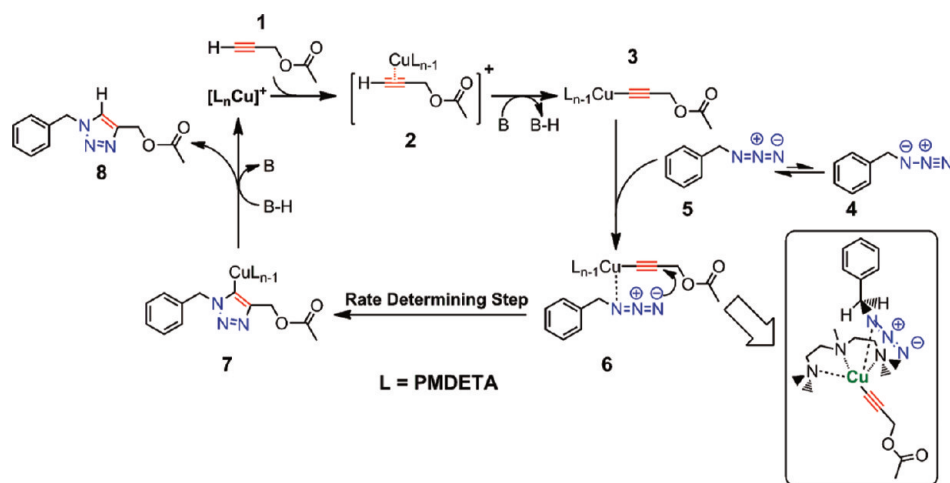


Figure 2. (a) Scores plot and (b) scatter scores plot of the first two principal components calculated from PCA on mean-centered online IR spectra with 1:1 molar ratio of azide and alkyne; (c) spectra comparison between loading plots of PC-1 and IR spectrum of pure triazole as well as (d) between PC-2 and pure azide and alkyne derived from experimental purification. The first two principal components explain 98% of the variation.

SCHEME 2: Modified Catalytic Cycle for Cu(I)-Catalyzed Azide–Alkyne Cycloaddition Reaction According to Infrared Correlation Analysis Results



score changes, while the formation of PC-1 or 1,2,3-triazole slowed. On the basis of the above analysis, we can easily confirm the rate-determining step to be the transition of the intermediate 1:1 complex of two reactants to the product 1,2,3-triazole.

To further examine the variation sequence of all reacting species, the three spectral regions in Figure 1b–d were all used to perform 2D correlation analysis, as shown in Figure 3. Synchronous spectra reflect simultaneous changes between two given wavenumbers. From Figure 3a, we can see an obvious band splitting of C=O at 1763 and 1736 cm^{−1}, which was contributed from the reactant alkyne and the product 1,2,3-triazole, respectively. Interestingly, asynchronous spectra had

distinguished the azido stretching vibration to three peaks at 2125, 2098, and 2079 cm^{−1}. Because an obvious shoulder peak can also be found in the IR spectrum of pure azide without Cu(I) (see Supporting Information for spectral comparison), we are inclined to assign these two peaks at 2125 and 2079 cm^{−1} to the two asymmetric N=N stretching vibrations of the azido resonance structure $-\text{N}=\text{N}^+=\text{N}^-$ and the peak at 2098 cm^{−1} to the single asymmetric N≡N stretching vibration of the other azido resonance structure $-\text{N}^--\text{N}^+=\text{N}$. Additionally, C–H stretching of alkyne exhibited two splitting bands at 3224 and 3182 cm^{−1}, which can be assigned to free $\equiv\text{C}-\text{H}$ and $\equiv\text{C}-\text{H}$ coordinated with Cu(I), respectively.

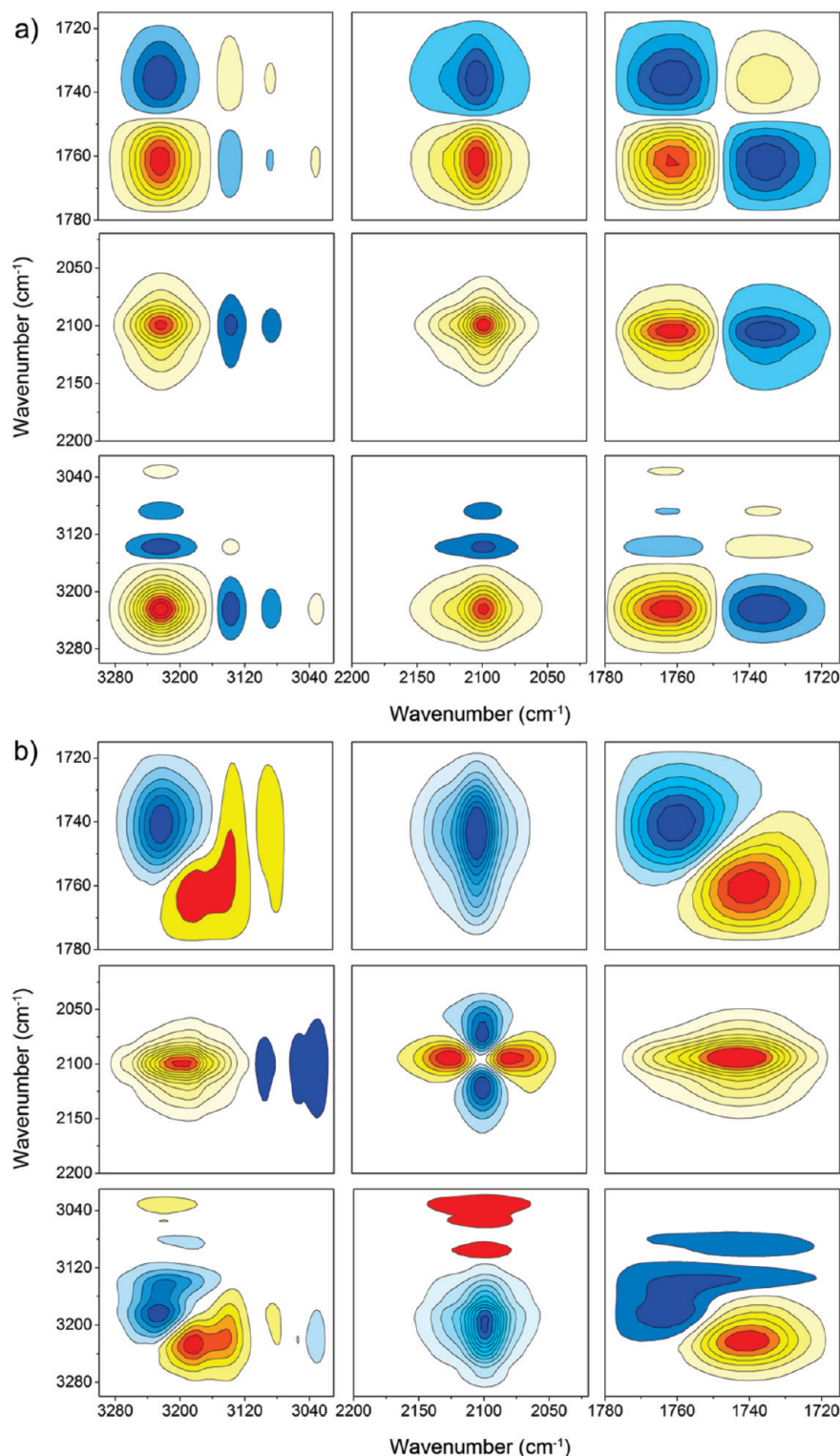


Figure 3. Two-dimensional (a) synchronous and (b) asynchronous spectra of the three spectra regions (3300–3010, 2200–2020, and 1780–1715 cm^{-1}) generated from online IR spectra with 1:1 molar ratio of azide and alkyne in the period of 0–30 min. Warm colors (red and yellow) are defined as positive intensities, while cool colors (blue) are negative ones.

The sequence can be determined according to Noda's rule,¹³ which can be summarized as follows: if the cross-peaks (ν_1 , ν_2 , and assume $\nu_1 > \nu_2$) in synchronous and asynchronous spectra have the same sign, the change at ν_1 may occur prior to that of ν_2 , and vice versa. The operation details for determination of sequence order according to a simplified method¹⁵ can also be found in Supporting Information, and only the final specific orders are presented here for all reacting species in the CuAAC reaction (\rightarrow means prior to or earlier than): 3182 \rightarrow 3224, 1763

\rightarrow 2125, 2079 \rightarrow 2098 \rightarrow 3086 \rightarrow 3139 \rightarrow 3032 \rightarrow 1736 cm^{-1} , e.g., $\equiv\text{C}-\text{H}$ (coordinated with Cu(I)) \rightarrow $\equiv\text{C}-\text{H}$ (free), $\text{C}=\text{O}$ (alkyne) \rightarrow $-\text{N}=\text{N}^+=\text{N}^-$ \rightarrow $-\text{N}=\text{N}^+=\text{N}^-$ \rightarrow phenyl \rightarrow C–H (triazole) \rightarrow C=O (triazole). From the sequence derived from 2Dcos, we can clearly find that the consumption of alkyne is earlier than azide followed by the formation of the product 1,2,3-triazole, which is consistent with our previous analysis.

For the convenience of description, the sequence has been presented in Scheme 2, in which some modifications on the

basis of the catalytic cycle proposed by Sharpless have been made, wherein it is noted that the consumption of Cu(I)-coordinated alkyne **2** was earlier than that of free alkyne **1**, contrary to the reacting direction. That is because the coordination of Cu(I) and alkyne to afford Cu(I) acetylide **3** proceeded very fast and 2Dcos cannot discern this sequence. The sequence between the two azido resonance structures of $\text{--N=N}^+=\text{N}^-$ **5** and $\text{N}=\text{N}^+=\text{N}^-$ **4** is also very meaningful in that it was the resonance structure $\text{--N=N}^+=\text{N}^-$ **5** that participates in the complexation between azide and alkyne. It is presumed that the coordination of Cu(I) acetylide to **5** may lead to a relatively lower activation energy in the following rate-determining step from the perspective of charge distribution. Along with the formation of 1,2,3-triazole **8**, phenyl and C=O were affected successively, with C=O being the slowest response. According to the catalytic cycle proposed by Sharpless, the azide-alkyne 1:1 complex **6** would first produce a preproduct or triazolyl-copper derivative **7** followed by its proteolysis to afford 1,2,3-triazole **8**. The slowest response of C=O in triazole indicates that this proteolysis process was also very fast and 2Dcos cannot discern it. Thus, the rate-determining step can be easily confirmed only to the transition of azide-alkyne 1:1 complex **6** to the preproduct **7**. This is the first experimental proof for the rate-determining step of the CuAAC reaction. In Scheme 2, the structure of azide-alkyne 1:1 complex **6** has also been presented according to a previous report.^{6a}

4. Conclusion

A designed ligand-accelerated CuAAC reaction was monitored for the first time by real time infrared analysis technique based on ATR-FTIR principles. Three reacting groups directly participating in the reaction (azido, alkynyl, and 1,2,3-triazole) are all IR-responsive and can be traced primely. The absorbance-time curves with different molar ratios of reactants as well as PCA calculations on the fingerprint region showed that the consumption of alkyne and azide took place successively followed by the formation of the product 1,2,3-triazole, and a 1:1 complex of two reactants or the intermediate would be formed in the reaction process, in good conformity with current catalytic mechanism that Sharpless proposed. 2Dcos discerned the sequence of all the reacting species and confirmed the rate-determining step of CuAAC reaction to be the transition of the azide-alkyne 1:1 complex to the preproduct 1,2,3-triazole. A modified catalytic cycle has also been plotted to get a better understanding of the CuAAC reaction.

Acknowledgment. We gratefully acknowledge the financial support National Science Foundation of China (NSFC) (20934002, 20774022), the National Basic Research Program of China (Nos. 2005CB623800, 2009CB930000).

Supporting Information Available: Determination of rate orders, operation details of sequence order determination from 2Dcos results, spectral comparison of azido vibrations. This material is available free of charge via the Internet at <http://pubs.acs.org>.

References and Notes

- (1) (a) Moses, J. E.; Moorhouse, A. D. *Chem. Soc. Rev.* **2007**, *36*, 1249. (b) Candeias, N. R.; Branco, L. C.; P. Gois, P. M.; Afonso, C. A. M.; Trindade, A. F. *Chem. Rev.* **2009**, *109*, 2703. (c) Kolb, H. C.; Finn, M. G.; Sharpless, K. B. *Angew. Chem., Int. Ed.* **2001**, *40*, 2004.
- (2) (a) Rostovtsev, V. V.; Green, L. G.; Fokin, V. V.; Sharpless, K. B. *Angew. Chem., Int. Ed.* **2002**, *41*, 2596. (b) Tornøe, C. W.; Christensen, C.; Meldal, M. *J. Org. Chem.* **2002**, *67*, 3057.
- (3) Himo, F.; Lovell, T.; Hilgraf, R.; Rostovtsev, V.; Noodleman, L.; Sharpless, K.; Fokin, V. *J. Am. Chem. Soc.* **2005**, *127*, 210.
- (4) (a) Singh, I.; Vyle, J. S.; Heaney, F. *Chem. Commun.* **2009**, 3276. (b) Zhou, Z.; Fahrni, C. *J. Am. Chem. Soc.* **2004**, *126*, 8862. (c) Nandivada, H.; Jiang, X.; Lahann, J. *Adv. Mater.* **2007**, *19*, 2197. (d) Zhang, Y.; He, H.; Gao, C. *Macromolecules* **2008**, *41*, 9581. (e) Fournier, D.; Hoogenboom, R.; Schubert, U. *Chem. Soc. Rev.* **2007**, *36*, 1369.
- (5) Rodionov, V. O.; Fokin, V. V.; Finn, M. G. *Angew. Chem., Int. Ed.* **2005**, *44*, 2210.
- (6) (a) Meng, J.-C.; Fokin, V. V.; Finn, M. G. *Tetrahedron Lett.* **2005**, *46*, 4543. (b) Rodionov, V. O.; Presolski, S. I.; Diaz Diaz, D.; Fokin, V. V.; Finn, M. G. *J. Am. Chem. Soc.* **2007**, *129*, 12705.
- (7) Punna, S.; Kuzelka, J.; Wang, Q.; Finn, M. *Angew. Chem., Int. Ed.* **2005**, *44*, 2215.
- (8) Binauld, S.; Boisson, F.; Hamaide, T.; Pascault, J.-P.; Drockenmüller, E.; Fleury, E. *J. Polym. Sci., Part A: Polym. Chem.* **2008**, *46*, 5506.
- (9) Himo, F.; Lovell, T.; Hilgraf, R.; Rostovtsev, V. V.; Noodleman, L.; Sharpless, K. B.; Fokin, V. V. *J. Am. Chem. Soc.* **2004**, *127*, 210.
- (10) Gandini, A.; Coelho, D.; Silvestre, A. J. D. *Eur. Polym. J.* **2008**, *44*, 4029.
- (11) (a) Thibault-Starzyk, F.; Seguin, E.; Thomas, S.; Daturi, M.; Arnolds, H.; King, D. *Science* **2009**, *324*, 1048. (b) Zhang, J.; Sato, H.; Furukawa, T.; Tsuji, H.; Noda, I.; Ozaki, Y. *J. Phys. Chem. B* **2006**, *110*, 24463. (c) Aggarwal, V.; Sheldon, C.; Macdonald, G.; Martin, W. *J. Am. Chem. Soc.* **2002**, *124*, 10300. (d) Owusu-Adom, K.; Schall, J.; Guymon, C. *Macromolecules* **2009**, *42*, 3275.
- (12) Hotelling, H. *J. Educ. Psychol.* **1933**, *24*, 417.
- (13) (a) Noda, I. *Bull. Am. Phys. Soc.* **1986**, *31*, 520. (b) Noda, I. *J. Am. Chem. Soc.* **1989**, *111*, 8116.
- (14) Kasuga, Y.; Onoda, W.; Ito, M.; Nakamura, Y.; Inokuma, S.; Matsuda, T.; Nishimura, J. *Heterocycles* **2009**, *78*, 983.
- (15) Sun, S.; Tang, H.; Wu, P.; Wan, X. *Phys. Chem. Chem. Phys.* **2009**, *11*, 9861.

JP105034M